

Stability of Ferric Oxide Hydrosols

BY F. DUMONT AND A. WATILLON

Université Libre de Bruxelles, Belgique

Received 3rd June, 1971

Ferric oxide hydrosols are composed of a haematite core surrounded by an hydrated oxide shell. Interactions have been studied, on both sides of the p.z.c., between ferric oxide surface and a series of anions and cations having characteristics ranging from structure promoters to structure breakers. Although ferric oxide has a moderate crystalline field, the observed adsorption sequences show that the interface acts as a structure promoter for water molecules. The large spreading of the measured adsorption sequences, especially at extreme pH values, proved the coagulation technique to be a good tool for the study of ion-surface interactions. A new type of behaviour has been observed; at low surface potentials the ions behave as indifferent but at higher surface potentials they are specifically adsorbed.

The properties of the ferric oxide/water interface have essentially been deduced from absorption isotherm determinations. Parks and De Bruyn¹ have shown that the potential-determining ions are H^+ and OH^- . The surface charge is due either to their adsorption on the superficial MOH groups or to dissociation of the latter. From the kinetics of this adsorption, Onoda and De Bruyn² have demonstrated the existence of two steps: the first is rapid and is due to the adsorption of the p.d.i. at the solid/liquid interface; the second is slow and caused by the diffusion of protons into or from a superficial shell of hydrated oxide surrounding a haematite core. Atkinson, Posner and Quirk³ have studied the rapid adsorption isotherms and have shown that the double-layer theory can reasonably be applied to the hydrated oxide/solution interface.

Our investigation represents an attempt to study the same problem by another approach, viz., the kinetics of coagulation of ferric oxide hydrosols in presence of various monovalent ions in the pH range 2-12.5.

EXPERIMENTAL

PREPARATION OF FERRIC OXIDE HYDROSOLS

The preparation of ferric oxide hydrosols comprises two consecutive steps, the precipitation of $Fe(OH)_3$ and the dehydration-aging of the hydroxide by heating. A preliminary series of hydrosols has been prepared using the Parks and De Bruyn¹ method, viz., hydrolysis at 100°C of a 0.05 M ferric nitrate solution, followed by two weeks aging at the same temperature. The latter operation has been performed at pH 1, 2, 3 and 4. We observed that the systems aged at pH 3 and 4 consisted of small yellow particles essentially composed of goethite, although sols aged at pH 1 and 2 comprised larger red-brick coloured haematite particles.⁴ Finally, we prepared a batch of sol precipitated and aged at pH 1.6. This value is high enough to prevent coagulation during aging but nevertheless low enough to promote haematite formation. The major part of the system was first centrifuged and the supernatant discarded. Finally, by moderate centrifugation, the larger aggregates were eliminated. The process was repeated a few times and controlled spectrophotometrically.

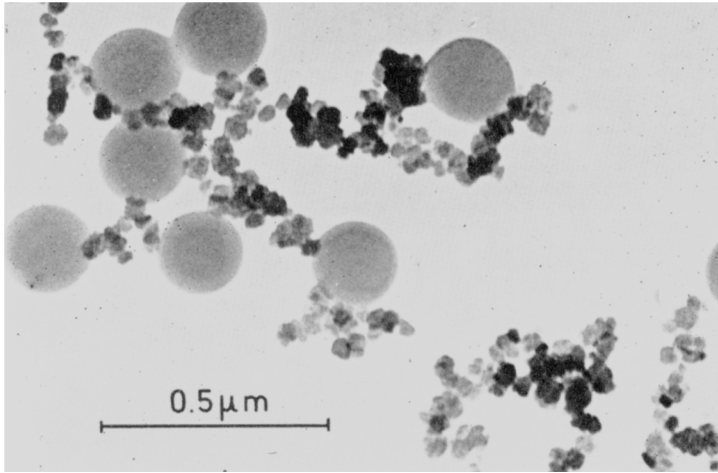


FIG. 1.—Electron micrograph of a fractionized sol; standard : DOW PSL LS O55A.

CHARACTERIZATION OF THE SYSTEM

Electron micrographs of the sol have been obtained, using a JEOL electron microscope, type JEM 120. Fig. 1 shows that the shape, which is reasonably symmetrical, can as a first approximation, be considered as spherical; the size standard is the Dow Polystyrene Latex LSO55A ($D = 188$ nm).

Using the semi-automatic Zeiss TGZ3 analyser and measuring 900 particles, the size histogram of fig. 2 has been established. The standard deviation has been estimated to be $\sigma = 0.12$. A number average diameter of 47.5 nm and a mean surface diameter of 47.9 nm have also been deduced. From the latter, we obtained a specific area, $S = 2.45 \times 10^5$ cm²/g. This value, determined on a fractionized sol, is in the same range as the values obtained with the B.E.T. method on some similar materials ($4.46 > S > 2.2 \times 10^5$ cm²/g).³

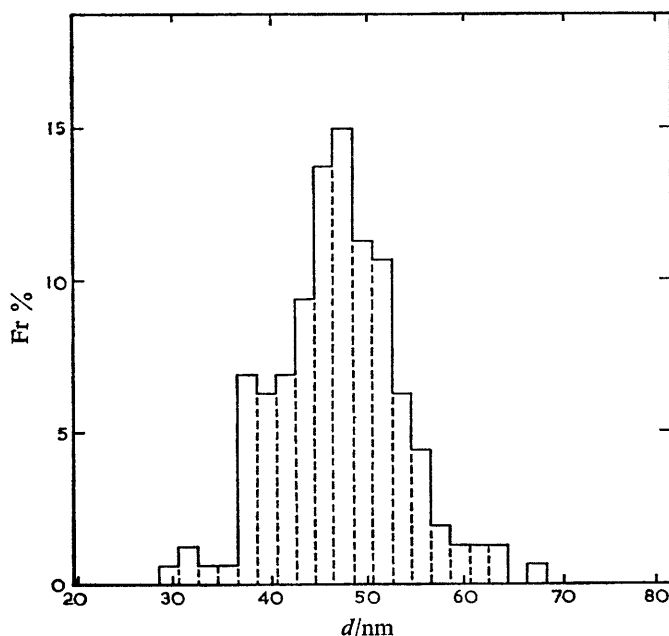


FIG. 2.—Size histogram of the fractionized sol.

In another approach, physisorbed water has been removed from a sample by prolonged outgassing at room temperature.⁵ Then, using a Chevenard balance, the water loss between 75 and 1000°C has been estimated as 3.02 % of the solid weight. Zettlemoyer and MacCafferty,⁶ from heats of immersion of haematite outgassed at different temperatures, concluded that water chemisorbed on the oxide represents a surface coverage of 5.88 OH⁻/nm²; desorption of these commences at 75°C. This corresponds, in our case, to a water loss from this cause, of 0.22 % of the sample weight. From the difference between the total weight loss and the latter, 2.8 % of weight is due to dehydration of the hydrated haematite shell. Furthermore, density determinations on the sol and dry weights after prolonged outgassing at room temperature lead to a particle density of $d = 4.870 \pm 0.007$.

Some hypothesis has now to be proposed, since the stoichiometric composition of this layer is not known. If the hydration water is assumed to be localized in a goethite-like layer (goethite: $\text{Fe}_2\text{O}_3 \cdot \text{H}_2\text{O}$, $d = 4.28$; haematite: Fe_2O_3 , $d = 5.24$), the hydration shell should have a thickness of about $\delta = 34$ Å. However, the probability that the surface shell is composed of goethite is low, because our X-Ray patterns, according to the Onoda and De Bruyn data,² failed to show any goethite in the particles, although the volume of the hydrated shell represents an appreciable fraction of the particle. The fact that Atkinson, Posner and Quirk³ have detected small amounts of goethite is probably related to the fact

that they dried their samples for 24 h at 110°C, a procedure which presumably involves some recrystallization of the hydrated oxide. In our case, for the same water content, we might therefore expect a thinner but more highly hydrated layer. As an example, a thickness of $\delta = 17 \text{ \AA}$ corresponds to the hydrated form $\text{Fe}_2\text{O}_3 \cdot 2.8\text{H}_2\text{O}$.

From the exchange of tritiated water between hydrated haematite and solution, Bérubé, Onoda and De Bruyn,² expressing the hydration thickness in terms of a goethite layer, obtained $\delta = 13.3 \text{ \AA}$. The difference between this value and ours can be assigned either to an overestimation of the surface area by the B.E.T. method, or to an underestimation in our determination in which we approximated our particles to spheres.

Nevertheless, it seems more realistic to assume that the hydration layer in the Bérubé *et al.* suspension is actually thinner than in our hydrosols because they aged the system at pH between 0 and 1. For stability, it has been necessary to carry out our aging process at pH 1.6.

DETERMINATION OF THE COAGULATION VALUES

The stability ratio W of a sol at a given electrolyte concentration is defined as the ratio between the rate of rapid coagulation of the sol and its coagulation rate at the considered electrolyte concentration. Verwey and Overbeek⁸ have shown that there is a linear relationship between $\log W$ and $\log C$ in the slow coagulation domain. Extrapolation of the experimental data to $\log W = 0$ allows us to determine the coagulation value C_{lim} .

We have previously shown⁹ that ferric oxide hydrosols obey the Rayleigh law at wavelengths longer than 600 nm. We therefore studied their kinetics of coagulation by the Troelstra¹⁰ method. The coagulation ratio of the system is directly related to the slope at the origin of the (extinction coefficients, time) plots.

The coagulations have been performed in the optical cell (length 5 cm) of a recording spectrophotometer Bausch and Lomb type Spectronic 505 at the wavelength $\lambda = 690 \text{ nm}$. The same volume of sol and of electrolyte were simultaneously injected through an Y-shaped fitting from two identical and parallel syringes, both actuated by the same driving motor. The injection rate was very reproducible and adjusted to be not shorter than 3 s, in order to avoid orthokinetic coagulation.

The pH after coagulation has been controlled; for pH higher than 5, care was taken to

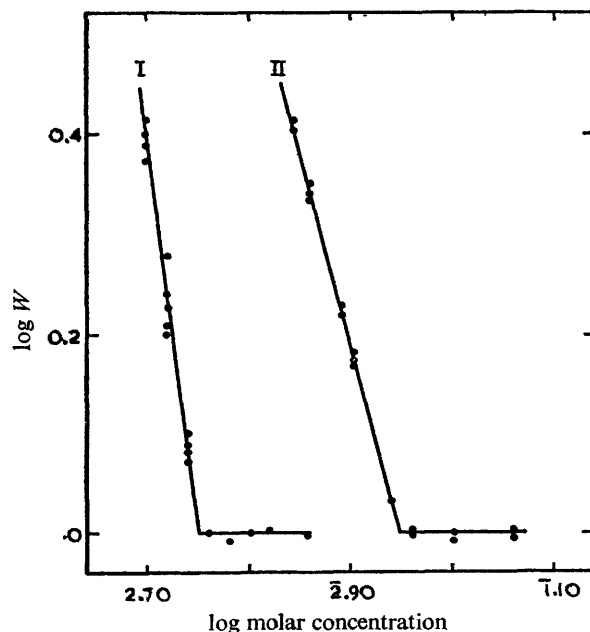


FIG. 3.—Dependence of the rate of coagulation on the electrolyte concentration; (I) pH 11, 8 counterion K^+ ; (II) pH 4, counterion ClO_4^- .

avoid CO_2 contamination. Fig. 3 shows as an example, $(\log W, \log C)$ curves obtained with a positive sol at pH 4 in presence of ClO_4^- as counterion, and with a negative sol at pH 11.8, with K^+ as counterion. The reproducibility of the determined C_{lim} is always better than 3 %.

In view of the existence of rapid and slow adsorption isotherms, before undertaking a systematic coagulation study, sol samples have been equilibrated for months at pH 2 and 6 respectively, after which coagulation has been studied on both systems at pH 2, 3 and 4, using ClO_4^- as counterion. The results are summarized on table 1. The lack of significant shifts of C_{lim} with equilibration pH, and the reproducible response to the bulk pH, indicate that the equilibrium between the hydrated oxide surface and the solution has been achieved for the conditions of our experiments, the coagulation time ranging between 20 and 100 s. Furthermore, the amount of protons adsorbed into the hydrated oxide layer does not seem to affect the stability of the sol, at least in the pH range studied, with the technique previously described.

TABLE 1.—COAGULATION BY ClO_4^-

pH of storage	pH of coagulation	C_{lim} , mM
6	2	154
2	2	154
6	3	135
2	3	137
6	4	106
2	4	103

RESULTS

In view of the necessity of maintaining stability, the sols have been stored at pH 6-6.5. Coagulation values have been determined for a series of monovalent ions

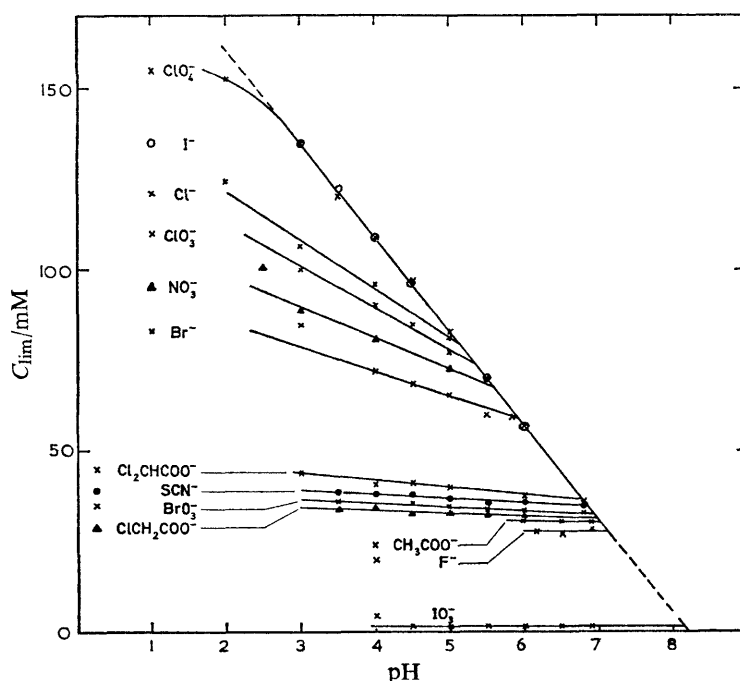


FIG. 4.—Coagulation values against pH for various anions.

in the pH range 2-12.5. The results are plotted on fig. 4 and 5. For the acid branch we used the Na^+ salts of the various anions studied. Except for Cl^- , NO_3^- , Br^- , CH_3COO^- , $\text{CH}_2\text{ClCOO}^-$ and $\text{CHCl}_2\text{COO}^-$, for which the corresponding acids were available, the pH has been adjusted using HClO_4 . In these cases, we avoided ClO_4^- concentrations exceeding 10 % of that of the anion to be studied. This condition prohibits measurements at pH lower than 3 for these anions. For the weak bases F^- and CH_3COO^- , correction has been made for association. Finally, for I^- , we did not succeed in obtaining results at $\text{pH} < 3$; below this point, it seems that the oxidation of I^- by the dissolved oxygen is catalyzed by the surface. At pH 6.85, coagulations have been studied in presence of various concentrations of a $\text{PO}_4\text{H}^{2-} + \text{PO}_4\text{H}_2^-$ buffer and extrapolated to zero buffer concentration.

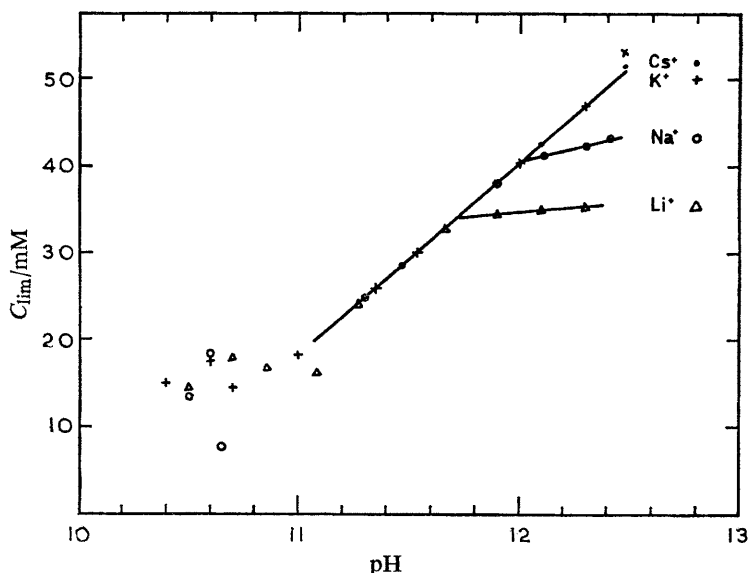


FIG. 5.—Coagulation values against pH for various cations.

In the alkaline region, the chlorides have systematically been used, the pH being adjusted by the corresponding hydroxides. It was not possible to store negative stable sols at pH 9-10. For every experiment, we therefore decided to reverse the charge of the sol stored at pH 6-6.5. However, the results were quite inaccurate at a coagulation pH lower than 11.

The extrapolation of the coagulation values against pH to $C_{\text{lim}} = 0$ in the acid region allowed us to locate the p.z.c. of our hydrated haematite at pH 8.2. Extrapolation from the alkaline region is imprecise but seems to indicate slightly higher values. At any rate, these estimations are in agreement with the data ranging between pH 8 and 9.4 reported by Parks¹¹ for the same material.

DISCUSSION

THE IONIC ADSORPTION SEQUENCES

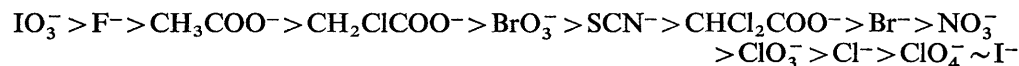
In electrolyte solutions, according to Gurney,¹² there are two different types of ion-ion interactions. The first occurs between two similar ions both having a high electrostatic field and which are therefore structure promoters for surrounding water molecules. The second type of interaction is observed between large ions with a

relatively weak field strength and which are less heavily hydrated, and therefore act even as structure breakers. A similar duality exists when one of the two species is a charged surface in equilibrium with an electrolyte solution.

Bérubé and De Bruyn,¹³ from adsorption of monovalent ions on TiO_2 suspensions, have proposed a model for this oxide/water interface. The OH superficial groups firmly anchor the neighbouring water molecules by hydrogen bonding, this phenomenon being strengthened by the large crystalline field of the Ti^{4+} ion. It results in a layer of "frozen" water near the surface, the latter behaving as a structure promoter macro-ion.

The effect of the crystalline field strength on the structuring properties of an interface has been emphasized by Stumm, Huang and Jenkins.¹⁴ In their work, two species of manganese dioxide present opposite adsorption series; for $\delta\text{-MnO}_2$ the order is $\text{Cs}^+ > \text{Na}^+$ and for $\beta\text{-MnO}_2$, $\text{Na}^+ < \text{Cs}^+$. In the first case, the surface behaves as a structure breaker and as a structure promoter in the second one. In close agreement with those observations, the field strength is low for $\delta\text{-MnO}_2$ (volume of the unit cell per central ion, $V = 44 \text{ \AA}^3$) and high for $\beta\text{-MnO}_2$ ($V = 27.6 \text{ \AA}^3$). Similarly, for AgI ($V = 54 \text{ \AA}^3$), the sequence $\text{Rb}^+ > \text{K}^+ > \text{Na}^+ > \text{Li}^+$ is obtained from adsorption isotherms by Lyklema¹⁵ and from the kinetics of coagulation by Kruyt and Klompé.¹⁶ For TiO_2 ($V = 26.2 \text{ \AA}^3$), the inverse series has been previously reported.¹³ For Fe_2O_3 , ($V = 35 \text{ \AA}^3$), the field strength has an intermediate value. This is confirmed by the fact that physisorbed water can be out-gassed from $\alpha\text{-Fe}_2\text{O}_3$ at 25°C although it can only be achieved for TiO_2 at $150\text{--}200^\circ\text{C}$ ¹.

A low coagulation value indicates a large specific adsorption, at extreme pH values, and the following adsorption sequences have been developed. In acidic media,



and in alkaline media, $\text{Li}^+ > \text{Na}^+ > \text{K}^+ \sim \text{Cs}^+$. The general trend is thus clearly indicated; the most structure promoting ions are the most strongly adsorbed while the typical structure breakers are not.

On the one hand, ClO_4^- seems, on the higher pH scale, to be non-specifically adsorbed; on the other, IO_3^- , although relatively large in size, has so weak I=O bindings that oxygen atoms can exchange very rapidly with those of water.¹⁸ IO_3^- behaves thus like a small ion, with its structuring properties explaining the large specific adsorption observed.

The drastic difference between ClO_4^- and IO_3^- at pH 3 is shown by their coagulation values: $C_{\text{lim}}^{\text{ClO}_4^-} = 135 \text{ mM}$, $C_{\text{lim}}^{\text{IO}_3^-} = 2 \text{ mM}$. It is thus clearly shown that the $\alpha\text{-Fe}_2\text{O}_3 \cdot \text{H}_2\text{O}$ behaves, despite the intermediate value of the field strength, as a structure-promoting surface.

On table 2, we compare the observed adsorption sequence on Fe_2O_3 with those measured on weak-acid¹⁹⁻²¹ and weak-base²² ion-exchange resins, which behave as structure promoting surfaces, and also to activity coefficients of the corresponding acids and bases²³ and to the B coefficients of viscosity²⁴ which reflect both ion-ion properties. Analogous series have been obtained in electrode kinetics by Gierst *et al.*²⁵

A reasonable parallelism between the various sequences is observed. Nevertheless, some discrepancies arise; e.g., SCN^- , which can undergo chemical binding with the Fe^{3+} ion, is more strongly adsorbed on ferric oxide than expected from previous considerations. Moreover CH_2ClOO^- and $\text{CHCl}_2\text{COO}^-$, structure breakers, are specifically adsorbed in acid media; the COO^- group which can organize water around itself is probably turned toward the surface.

TABLE 2.—THE IONIC ADSORPTION SEQUENCE

- (1) Sequence found in this work on $\text{Fe}_2\text{O}_3 \cdot \text{H}_2\text{O}$.
 (2) Activity coefficient of corresponding acid or hydroxide.
 (3) B coefficients of viscosity.
 (4) Sequences on Dowex 2 for anions, on Amberlite IRC 50 for cations.

(1)	(2)	(3)	(4)
$\text{ClO}_4^-(\text{I}^-)$	HI HBr HClO_4	I^- ClO_4^-	ClO_4^- SCN^- I^-
Cl^- ClO_3^- NO_3^- Br^-	HCl HNO_3	NO_3^- Br^- ClO_3^-	NO_3^- Br^-
$\text{CHCl}_2\text{COO}^-$		Cl^-	$\text{CHCl}_2\text{COO}^-$ Cl^-
SCN^- BrO_3^- $\text{Cl}_2\text{CHCOO}^-$			BrO_3^- $\text{Cl}_2\text{CHCOO}^-$ IO_3^-
CH_3COO^- F^- IO_3^-		F^- IO_3^-	CH_3COO^- F^-
Cs^+K^+	CsOH KOH	Cs^+ K^+	Cs^+ K^+
Na^+	NaOH	Na^+	Na^+
Li^+	LiOH	Li^+	Li^+

THE POTENTIAL Ψ_δ AT COAGULATION

The calculation of ψ_δ for coagulation requires the combination of the Van der Waals-London attraction curve with the hypothetical Coulomb repulsion curve giving the first total interaction profile with no positive maximum. The attraction energy has been computed, by means of an I.B.M. 7040 Data Processing System, using the Hamaker-Vold^{26, 27} equation applied to a single surrounding shell and corrected for retardation propagation.²⁸ The Hamaker constant for haematite is $A_{\text{vacuum}}^{\text{Haem.}} = 15.2 \times 10^{-13}$ ergs.²⁹ For the hydrated layer, as a first approximation, we considered that the haematite and water contributions are proportional to their respective mol fractions. With a choosen shell thickness $\delta = 17 \text{ \AA}$ the composition $\text{Fe}_2\text{O}_3 \cdot 2.8\text{H}_2\text{O}$, $A_{\text{vacuum}}^{\text{hydr.ox.}} = 6.31 \times 10^{-13}$ ergs. The goethite-like shell hypothesis ($\text{Fe}_2\text{O}_3 \cdot \text{H}_2\text{O}$, $\delta = 34 \text{ \AA}$, $A_{\text{vacuum}}^{\text{Goeth.}} = 9.17 \times 10^{-13}$ ergs) gave similar results.

The interparticle electrostatic repulsion energy can be calculated when the potential of the Stern layer ψ_δ is low (the situation at coagulation) by means of the Derjaguin equation.³⁰ Combining the attraction curve and the appropriated repulsion one, using the above process, we deduced the ψ_δ values at coagulation. As an example, fig. 6 represents the interaction curves corresponding to coagulation at pH 3 by ClO_4^- and IO_3^- respectively. We obtained $\psi_\delta^{\text{coag.}}(\text{ClO}_4^-) = 30.2 \text{ mV}$, and $\psi_\delta^{\text{coag.}}(\text{IO}_3^-) = 10.3 \text{ mV}$. The interparticle distances corresponding to the interaction maximum are respectively 7 \AA for ClO_4^- and $80\text{--}100 \text{ \AA}$ for IO_3^- .

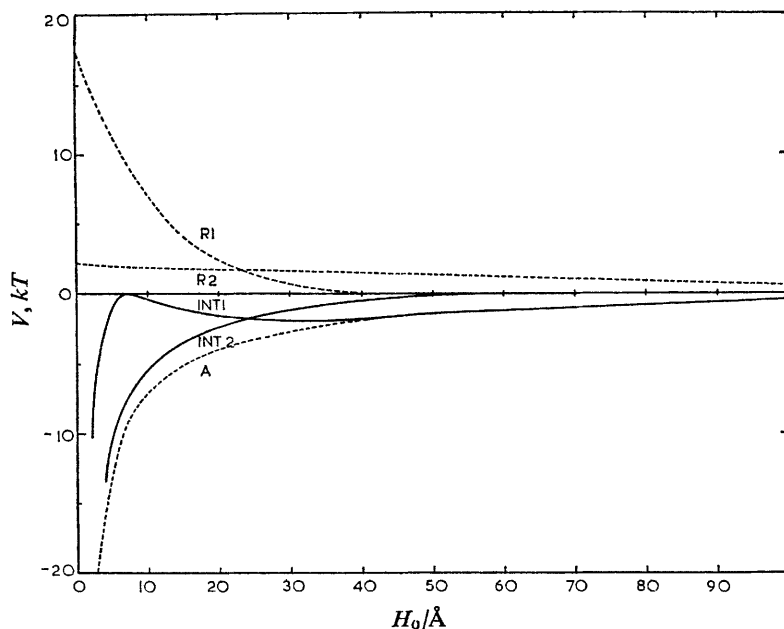


FIG. 6.—Combination of Van der Waals-London attraction and Coulomb repulsion at pH 3. A, attraction curve; R_1 , repulsion curve at coagulation by ClO_4^- ; Int_1 interaction curve at coagulation by ClO_4^- ; R_2 , repulsion curve at coagulation by IO_3^- ; Int_2 interaction curve at coagulation by IO_3^- .

By comparison with ClO_4^- , the specifically adsorbed IO_3^- displays a difference in behaviour; its coagulation value, about two powers of ten lower, indicates an important ionic adsorption at the surface. Therefore, at coagulation, which appears

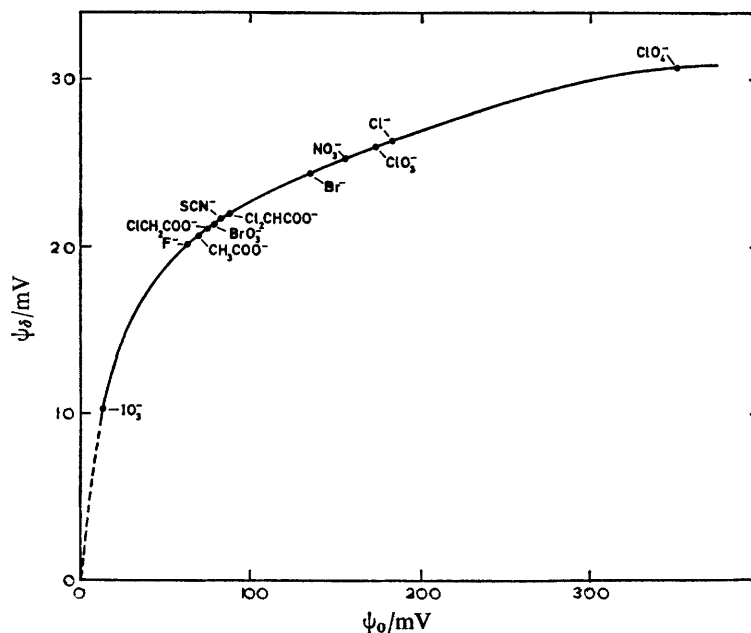


FIG. 7.— (ψ_0, ψ_δ) relationship corresponding to the specificity threshold for different anions.

at the same κH_0 value as that with ClO_4^- , the corresponding $1/\kappa$ characteristic Debye length is about 10 times lower. The Coulomb forces have thus a much larger range of action and at distances where they are still operative, the Van der Waals forces are considerably attenuated. Consequently, a small ψ_δ potential, as observed for IO_3^- , suffices to coagulate the system.

THE SPECIFICITY THRESHOLD

In fig. 4, minimum coagulation values, for which the ions depart from the general trend and begin to follow some specific behaviour, can be defined as their "specificity threshold". In fig. 7, the ψ_δ values corresponding to this threshold for various anions have been plotted against ψ_δ values, calculated assuming that the Nernst equation is obeyed at the ferric oxide water interface.³¹

These data suggest that for low ψ_0 potentials, the structured water at the interface maintains all the ions sufficiently far away from it so that they display a non-specific behaviour. With sufficiently large ψ_0 values, the electrostatic attraction becomes high enough to pull the ions through the structured layer, to the surface, where they become specifically adsorbed. With increasing threshold potentials, the ionic specificity sequence is in the order: strong structure promoters, low structure promoters, low structure breakers and strong structure breakers.

Our thanks are due to Prof. L. Gierst for many stimulating discussions.

¹ G. A. Parks and P. L. de Bruyn, *J. Phys. Chem.*, 1962, **66**, 967.

² G. Y. Onoda, Jr. and P. L. de Bruyn, *Surface Sci.*, 1966, **4**, 48.

³ R. J. Atkinson, A. M. Posner and J. P. Quirk, *J. Phys. Chem.*, 1967, **71**, 550.

⁴ H. B. Weiser, *Inorganic Colloid Chemistry*, (Wiley-New York, 1935), vol. 2, p. 40-44.

⁵ G. Blyholder and E. A. Richardson, *J. Phys. Chem.*, 1962, **66**, 2597.

⁶ A. C. Zettlemoyer and E. McCafferty, *Z. phys. Chem. (N.F.)*, 1969, **64**, 41.

⁷ Y. G. Bérubé, G. Y. Onoda, P. L. de Bruyn, *Surface Sci.*, 1967, **8**, 448.

⁸ E. J. W. Verwey and J. Th. G. Overbeek, *Theory of Stability of Lyophobic Colloids*, (Elsevier, 1948).

⁹ A. Watillon, L. Schoepen, J. Th. G. Overbeek, *Amer. Chem. Soc. Symp. Coagulation and Coagulant Aids*, (Los Angeles, 1963).

¹⁰ S. A. Troelstra and H. R. Kruyt, *Kolloid Beih.*, 1943, **54**, 225.

¹¹ G. A. Parks, *Chem. Rev.*, 1965, **65**, 177.

¹² R. W. Gurney, *Ionic Processes in Solution*, (Dover Publ., 1953).

¹³ Y. G. Bérubé and P. L. de Bruyn, *J. Colloid Sci.*, 1968, **28**, 92.

¹⁴ W. Stumm, C. P. Huang and S. R. Jenkins, *Croat. Chem. Acta*, 1970, **42**, 223.

¹⁵ J. Lijklema, *Trans. Faraday Soc.*, 1963, **59**, 418.

¹⁶ H. R. Kruyt and M. A. M. Klompé, *Kolloid Beih.*, 1942, **54**, 484.

¹⁷ J. J. Jurinak, *J. Colloid Sci.*, 1964, **19**, 477.

¹⁸ E. Nightingale, *J. Phys. Chem.*, 1960, **64**, 162.

¹⁹ J. I. Bregman, *Ann. N.Y. Acad. Sci.*, 1953, **57**, 125.

²⁰ C. E. Marshall and G. Garcia, *J. Phys. Chem.*, 1959, **63**, 1663.

²¹ H. P. Grégor, M. J. Hamilton, R. J. Oza and F. Bernstein, *J. Phys. Chem.*, 1956, **60**, 266.

²² R. Kunin, *Ion Exchange Resins*, (Wiley, 1963), p. 62.

²³ R. A. Robinson and R. H. Stokes, *Electrolyte Solutions*, (Butterworth, London, 1959).

²⁴ E. R. Nightingale, Jr. in *Chemical Physics of Ionic Solution*, B. E. Conway and R. G. Barradas ed., (Wiley, New York, 1964), p. 87.

²⁵ L. Gierst, E. Nicolas and L. Tytgat-Vandenberghen, *Croat. Chem. Acta*, 1970, **42**, 117.

²⁶ H. C. Hamaker, *Physica*, 1937, **4**, 1058.

²⁷ M. J. Vold, *J. Colloid Sci.*, 1961, **16**, 1.

²⁸ H. R. Kruyt, *Colloid Science*, (Elsevier, 1952), p. 271.

²⁹ F. Fowkes, *Ind. Eng. Chem.*, 1964, **56**, 40.

³⁰ B. V. Derjaguin, *Acta Physicochim.*, 1939, **10**, 333.

³¹ Y. G. Bérubé and P. L. de Bruyn, *J. Colloid Sci.*, 1968, **27**, 305.